CSU Geospatial Review

GEOGRAPHIC INFORMATION SCIENCE IN THE CALIFORNIA STATE UNIVERSITY SYSTEM

VOLUME 19 • SUMMER 2023

ISSN 2373-5783

csugis.sfsu.edu

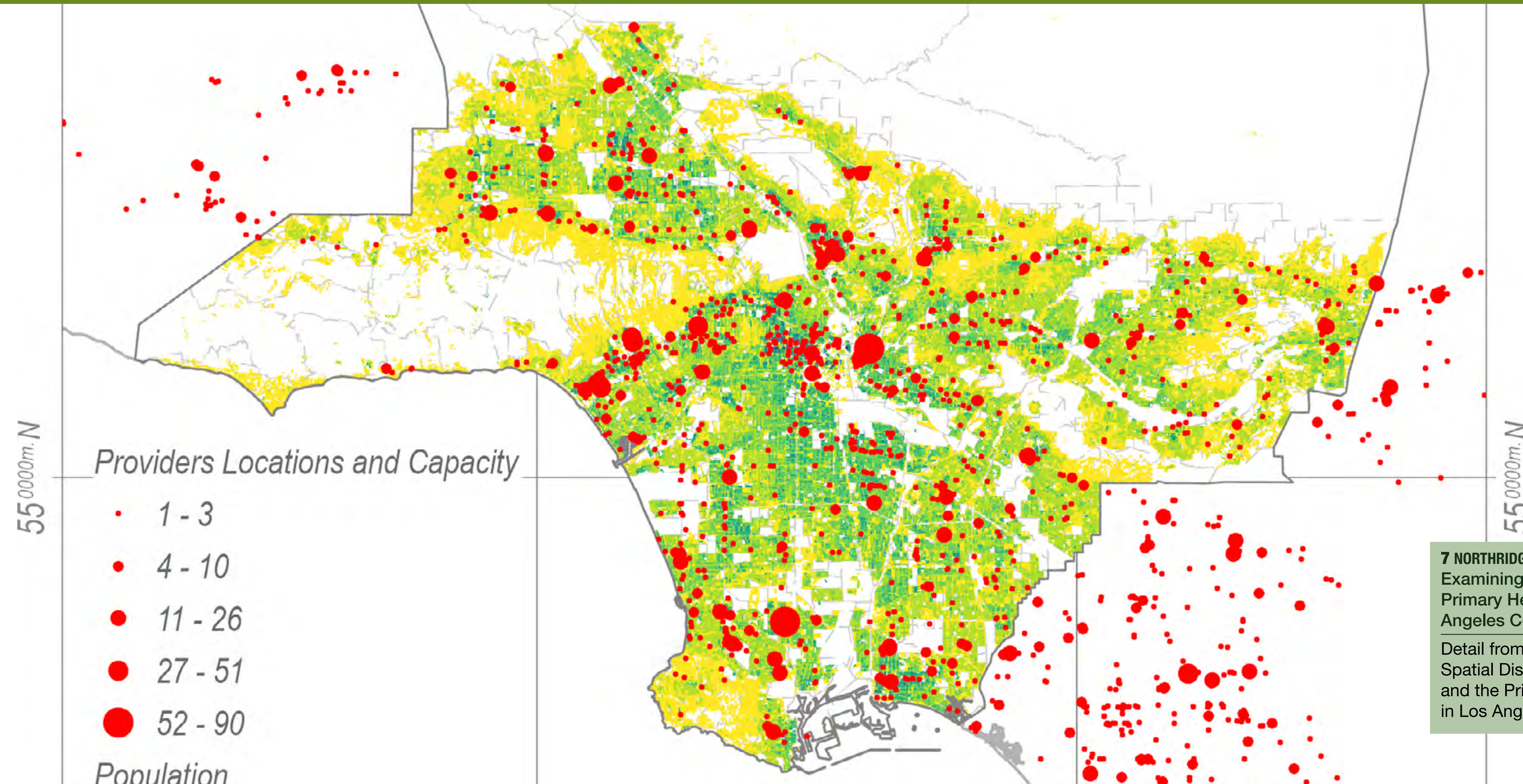

7 NORTHRIDGE
Examining Spatial Accessibility to Primary Healthcare Facilities in Los Angeles County

Detail from a map showing the Spatial Distribution of Population and the Primary Healthcare Centers in Los Angeles County.

INSIDE

Back to Normal?

We might have heard this before, but it's kind of feeling like we're getting back to normal, after a roller coaster ride during various waves of the pandemic. It finally sank in recently when giving a GIS class and being able to walk around the lab assisting students; suddenly it felt back to normal. We certainly learned some new tricks being forced to experiment with online tools, not just in the classroom but also for collaborative research, or even increasing attendance at research presentations with a Zoom option. And I've found that coding classes actually work better online, since it's easier to debug code. But for most classes, the personal connection we get when face to face is really important, and field research when having to isolate in separate vehicles never worked well.

Of course, nature (and social nature) has kept on throwing challenges and things to study our way. During the pandemic we've also gone through a major drought with record wildfires. And now we're watching record snow accumulations melt, probably leading to record flooding. The interplay of multiple geographic systems at multiple scales is providing no end of puzzles to solve. As a geomorphologist, I'm pretty excited to see the effects of fluvial dynamism this summer, and am happy to have the tools to study, measure, and model the resulting landscapes.

Jerry Davis, Director, CSU GIS Specialty Center
San Francisco State University

Monitoring Bull Kelp Growth in a Farm System Using an Unoccupied Aerial Vehicle

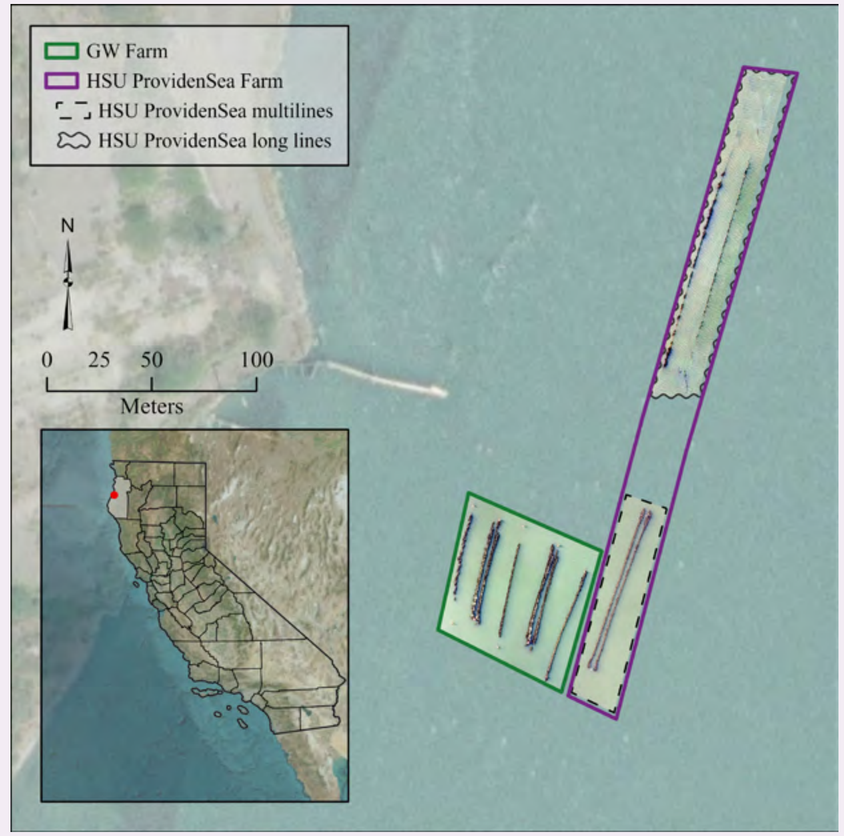

Figure 1: Configuration of the two kelp farms in Humboldt Bay, in northern California.

Bull kelp *(Nereocystis leutkeana)* is a staple seaweed along the west coast of North America, providing habitat and resources for nearshore fisheries and carbon-rich debris when strong storms dislodge the kelp and transport it to the deep sea or upon beaches (Graham, Dayton, and Erlandson 2003; Springer et al. 2007). In addition to ecological services, it has traditionally been harvested for food, fishing line, containers and other items by the First Peoples of the northwest (Turner 2001). Since 2015, there have been significant losses in kelp along the northern California coastline from marine heatwaves and the decline of urchin predators such as the sunflower sea star *(Pycnopodia helianthoides),* which has enabled booming urchin populations and relentless herbivory on the kelp (Rogers-Bennett and Catton 2019). To rebuild resilience in this region, many restoration strategies are ongoing, including the removal of urchins, transplanting kelp directly and limiting harvest (Gleason et al. 2021; Ward et al. 2022; Ray et al. 2022). Farming kelp offers another avenue to build resilience through removing harvest pressure on wild stock and introducing the nutrient-extractive properties of kelp to the locality (Kim et al. 2017).

The cultivation of bull kelp has been tried along the West Coast, mainly in Alaska (McDowell-Group 2017; Stopha 2020). These ocean farming techniques originated in Asia with various other seaweeds, but the practices have recently become prominent along the northeast coast of the United States (Kim et al. 2017). This growth has been expedited through the efforts of GreenWave, a non-profit organization based on the East Coast which provides training and tools to develop more regenerative ocean farms (GreenWave n.d.). The concept gained traction largely because it requires zero input of water or fertilizer, and it removes nutrients and carbon from the water (Duarte 2017; Chopin et al. 1999; Troell et al. 1999).

In Humboldt Bay, pre-permitted leases allowed for the establishment of two adjacent kelp farms, constituting the first open-water, commercial seaweed farms in the state. The first is owned by California Polytechnic University, Humboldt (originally name and hereafter, the "HSU ProvidenSea farm"), and the second is owned by GreenWave (GW, hereafter, the "GW farm") and operates in partnership with Hog Island Oyster Company, The Nature Conservancy, and Sunken Seaweed. Bull kelp growth in a bay setting has not been well documented and even cultivating the kelp on farms in Alaska has proved challenging (M. Stanley, personal communication, February 22, 2022). One of the major costs in farming is consistent in situ monitoring of the lines, which may be reduced with remote monitoring.

Our objective is to develop a cost-effective, high-resolution method of monitoring bull kelp growth in farm systems in a bay. To achieve this, we used Unoccupied Aerial Vehicle (UAV), also known as drones, to survey bull kelp farms in Humboldt Bay.

This study used imagery collected from UAV surveys over kelp farms in Humboldt Bay approximately every two weeks between March 10th and May 31st, 2022. The GW farm was seeded in early March 2022 and the HSU ProvidenSea farm was a few days later. The UAV used was a DJI Mavic 2 Pro with the standard, integrated Hasselblad camera. All the imagery used in this study were acquired in the visible spectrum (3-band) because use of color imagery (versus

continued on page 5

Analyzing Spatial Mismatch Of Domestic Violence Shelter Sites And Measuring Victim Costs From Misallocation

Click on any figure below to enlarge.

Figure 1: County Spatial Mismatch Index Scores Across California

Figure 2: County Aggregate Annual Domestic Violence Calls

Figure 3: County Aggregate Annual Emergency Domestic Violence Beds

It is eye-opening that far more animal shelters exist in the U.S. than shelters for battered women and their children; especially since domestic violence is the leading cause of homelessness for America's women and children (American Civil Liberties Union, 2005). Often, victims find that confidential shelters are full and standard homeless shelters are not equipped to deal with the sensitive needs and safety that domestic violence victims require.

In a one-day survey done in September 2019 from 96 participating shelter programs in California, there were 1,236 unmet requests for services due to a lack of resources available. Of these unmet requests, 51% (630) were for housing (National Network to End Domestic Violence, 2020). Many domestic violence victims depend on shelter services to escape their violent partners, which is why these resources play a vital role in victim outcomes. Therefore, it is important to analyze if shelters are placed efficiently for those in need. Ideally, the supply of services (beds available) should be geographically and proportionately matched with areas of demand (incident calls). Without much research on the geographic placement of shelter services for victims of domestic violence, this study seeks to explore how appropriately supply and demand of services are spatially matched across California. Domestic violence victim costs associated with any mismatch or misallocation of resources are then calculated to give perspective of the impact it can have on victims.

Data for this project were collected from several sources including but not limited to the California Department of Justice, U.S. Census Bureau, KidsData.org, and the Department of Housing and Urban Development (HUD). Variables include total domestic violence calls per city across California (2020), population census data (2020), and domestic violence emergency shelter locations with bed count data (2020). The mapped shelter locations are the public mailing addresses of the shelters, which is either their intake location or P.O. box. This location is within the same city as the shelter itself. However, the address location where victims are housed is kept confidential to ensure their safety and protection. A report from the California Research Bureau on the prevalence of domestic violence estimated that as of 2014 there were 112 emergency domestic violence shelters in California. This study includes 115 shelters, providing support that all shelters have been included. Using ERSI's ArcMap software, shelter locations with their corresponding annual number of available beds was mapped to model supply for services. Demand for services in each city was modeled using the annual number of incident calls to police. The data at the city level provide an intermediary step in the final analysis, described in more detail below. As such, the city data is not visualized in a map. However, to provide more general context for domestic violence across the state of California, the aggregate number of calls and shelter beds available are provided in Figure 2 and Figure 3.

Spatial mismatch theory began with the early works of John Kain (1964, 1968) to identify disparity between urban jobs and black residents. Spatial mismatch is defined in this research as the geographical separation between domestic violence victims and shelter services within city boundaries across counties. It is measured by the unevenness in the proportional distributions of the two. To calculate spatial mismatch, a modified version of the Dissimilarity Index was used. The Dissimilarity Index is often referred to as the Spatial Mismatch Index (SMI) due the fact it "is commonly used to measure spatial mismatch because it calculates the disproportionality of two groups in each areal unit of a city or metropolitan area" (Eom, 2022). The SMI has been applied to measure an abundance of disparities such as immigration, plant life, hazardous materials, and even irrigation topics. The formal equation for the dissimilarity index is:

$$\mathrm{D} = \frac{1}{2}\sum_i \left|\frac{x_i}{X} - \frac{y_i}{Y}\right|$$

Where $i = (1\ldots, n)$ refers to a given geographic areal unit, x_i and y_i are two groups of interest, and X and Y are the total sums of each group in a larger geographic area (Eom, 2022; Liu & Painter, 2011). The modified SMI equation used for this study is represented as:

$$\mathrm{SMI} = \frac{1}{2}\sum_i \left|\frac{S_i}{S} - \frac{V_i}{V}\right|$$

Where $i = (1\ldots, n)$ refers to the city (i) located within the larger geographic county unit; S_i is the number of victims housed by shelters in city (i); S is the number of victims housed by shelters in the corresponding county; V_i is the number of victims in city (i) measured by number of domestic violence calls; and V is the number of victims in the corresponding county.

As written, the SMI ranges between 0 (perfect balance) and 1 (perfect imbalance). Multiplying the SMI by 100 is interpreted as the percentage of either victims or shelters that would need to be relocated to achieve perfect balance in the distribution of services within the county. There are limitations with the use of the SMI since it does not consider the physical distance between shelters and victims—granted this is not an accessibility study and the aggregate call data does not allow for it. Rather, the SMI focuses on the proportional distribution among geographic subunits in a larger metropolitan area. In other words, the SMI measures the imbalance between supply and demand of shelter services across cities within each county. To take an extreme example, suppose that all victims resided in one city of a county while all shelters were in a different city. Whether these two cities are one mile apart from one another or 30 miles apart will not influence the index score. In both instances, the index for the county would be equal to 1, implying perfect imbalance. Nonetheless, as a summary measure, the SMI does allow uniform comparisons across geographic areas and has ease of interpretation.

Furthermore, it is important to remember that the supply of shelter services is far less than the demand for services in almost every county across California. However, the SMI is

continued on next page

TOC

not simply measuring whether each victim has a bed available to them. Rather, it is providing a measure of the proportionality of victims to shelter services. For example, within a given county if 15% of the total victims are in City A, then 15% of the shelter bed supply should also be City A. This ensures that all victims in the county have an efficient and equitable opportunity to receive services when they are proportionately distributed.

The analysis results give an SMI score for each county in California. These index scores are mapped in Figure 1. The counties in dark green represent the highest degree of spatial mismatch between demand and supply of domestic violence services, implying problematic areas, while the counties in light green show a proportionally adequate distribution of resources. Out of all 58 counties in California, eleven have a spatial mismatch index value of zero. For these counties, shelter services are in the same city/cities where calls for help were reported. Also, eight of the eleven counties have a greater annual supply of shelter beds than the number of calls for help. The three exceptions to this are San Francisco, Mariposa, and Sutter counties. In contrast, eight counties have a SMI value of one, representing perfect mismatch between domestic violence demand and shelter resources. Five of these seven counties had no shelters located within their borders (Alpine, Colusa, Mono, Sierra and Yuba) but did have calls for help. The other two counties, Calaveras and Plumas, had shelters but they were all located in a different city than where calls for help were reported. All of these counties are fairly small in terms of population and mainly rural, which may explain the lack of service supply coverage across the county. Besides the extreme cases of an SMI score of 0 or 1 described above, the counties with the lowest SMI scores include El Dorado (0.06), Tehama (0.10), Madera (0.13), Shasta (0.15), Santa Cruz (0.15), Napa (0.16), and Fresno (0.19). These counties have less than 20% of spatial mismatch occurring. Counties with high SMI scores include Placer (0.94), Lake (0.85), San Mateo (0.85), Contra Costa (0.83), San Bernardino (0.81), and Riverside (0.76). All of which have more than 75% of spatial mismatch occurring.

The main purpose of measuring the spatial mismatch is to calculate the number of “underserved” victims (i.e., those currently not appropriately or proportionately matched to services). This information is then used to estimate the economic costs victims may suffer because of the misallocation of resources in shelter placement. Victim cost data was originally sourced from a 1995 study on the health and productivity costs per victim, available from the Centers for Disease Control (CDC), and then updated to what current costs were in 2020. The total estimated costs from misallocation of domestic violence shelter services across California is estimated to be between $528 million and $629 million dollars. A summarized breakout of these direct costs is shown in Table 1. A full breakout of each cost category is available upon request.

	Low Estimate (27,664 victims)	High Estimate (66,661 victims)
Productivity Costs	21,131,275	53,444,443
Healthcare Costs	189,397,980	257,129,607
Loss of Life Costs	317,261,806	317,261,806
Total	**$527,791,061**	**$627,835,855**

Table 1: Estimated Victim Costs from Shelter Resource Mismatch

The implication of this study is that the spatial distribution of social services, specifically domestic violence shelter services, has real effects on society. When shelter services are not distributed efficiently, meaning proportionately matched to the demand for services in that area, victims in the mismatched areas are underserved and suffer the costs associated with domestic violence. Reducing these spatial mismatches between the supply and demand of resources can help reduce victim costs by ensuring victims have equitable opportunities to seek resources regardless of where they live. A potential solution for cities that do not have the current ability to expand shelters, may be to outsource services to safe places such as hospitals, secure hotels, or community living spaces. This may work especially well for rural areas where it is difficult, and perhaps inefficient, to provide multiple shelter sites across the region due to low population densities. Outsourcing the services would save on the startup and overhead costs needed to run a shelter, while still providing the security that victims need to get on their feet. Other counties with high degrees of spatial mismatch would better serve domestic violence victims by appropriately matching their shelter services to the demand within each city.

REFERENCES

American Civil Liberties Union. (2005). Domestic Violence and Homelessness Survey. American Civil Liberties Union.

California Partnership to End Domestic Violence. (2011). California Domestic Violence Fact Sheet. California Partnership to End Domestic Violence.

Centers for Disease Control and Prevention. (2003). Costs of Intimate Partner Violence Against Women in the United States. Atlanta: Center for Disease Control, National Center for Injury Prevention and Control.

Eom, H. (2022). Recent intra-metropolitan patterns of spatial mismatch: Implications for black suburbanization and the changing geography of mismatch. Growth and Change, 1– 25. https://doi.org/10.1111/grow.12653

Kain, J. F. (1964). The Effects of the Ghetto on the Distribution of Nonwhite Employment in Urban Areas. Washington DC: National Academic Press.

Kain, J. F. (1968). Housing Segregation, Negro Employment, and Metropolitan Decentralization. Quarterly Journal of Economics 82 , 1, 32-59.

Liu, C. Y., & Painter, G. (2011). Imigrant Settlement and employment Suburbanization in the US: Is There Spatial Mismatch? Urban Studies .National Network to End Domestic Violence, 2020. 14th Annual Domestic Violence Counts Report. Washington, DC. https://nnedv.org/content/domestic-violence-counts-14th-annual-census-report/

AUTHOR

Erica Freer
Economics Department
College of Humanities, Arts, Behavioral and Social Sciences
California State University, San Marcos

color-infrared) is thought to be more effective in penetrating water and detecting submerged kelp (Jensen, Estes, and Tinney 1980). The UAV was flown at an approximate altitude of 46 meters above ground level, to maximize both efficiency and resolution. The flight path, altitude, image overlap (80% front and side) and speed (11 kilometers per hour) were all preset in DroneDeploy Pro. Surveys were performed at opportune times, with ideal conditions including minimal wind, low and slack tide, low sun angle, and no low-lying fog (Joyce et al. 2019).

The UAV takes hundreds of individual images along the survey path at set distances to achieve the preset overlap. DroneDeploy Pro was used to process the images to build an orthomosaic, or a seamless image of the entire site, based on similar points, or "tie points" in the image. Based on conditions during the survey, the amount of kelp visible, floating items in the imagery, and several other factors, the resulting orthomosaic would sometimes have obvious defects. If so, the area with defects would be eliminated from the orthomosaic using geoprocessing tools in Esri's ArcGIS Pro (version 2.8.3; ArcGIS). In ArcGIS all the orthomosaics were further clipped to an extent directly surrounding the lines to reduce noise from surrounding water and other visible features.

To classify kelp from the UAV imagery, several classification methods were tried on one orthomosaic from May 31st, 2022. First, with the original red, blue, green (RGB) orthomosaic, we performed a supervised classification to separate the kelp from water, using a support vector machine algorithm (Huang, Davis, and Townshend 2002). To train the algorithm we provided manually digitized training samples of 3 classes: "water", "kelp", "buoy". Second, we ran an unsupervised classification, requesting 3 classes to be automatically generated based on distinguishing spectral signatures.

We also created an index from the original RGB orthomosaic subtracting the blue band from the red (Equation 1), as it was found by KC Cavanaugh to be the best in distinguishing kelp from seawater in RGB imagery (Cavanaugh et al. 2021). We applied the same supervised and unsupervised classifications to this new indexed orthomosaic. Then, we applied a binary threshold classification in which we tried a range of pixel values which best split the kelp and water according to a visual assessment of a histogram of the indexed orthomosaic's pixel values.

Equation 1. *Index = Red – Blue*

The accuracy assessment was performed in ArcGIS using 99 equalized stratified random points (N=33 per class). The classified results were assigned to each point. To build a reference dataset, we added the class that each point fell on based on the original RGB imagery. The performance differences between the classified results and these reference results were then computed with a confusion matrix. This matrix outputs three metrics, two of which were specific to accuracy within the kelp class. Producer accuracy is an indicator of false negatives while user accuracy indicates false positives of classified kelp. The third metric, the kappa statistic, provides a score representing the overall performance of the classification, including all three classes. The best performing classifier was selected and applied to all the other survey orthomosaics. The area of kelp classified on each line was calculated from the results of the classification. To determine variation in classified kelp resulting from the differing tidal condition across all surveys, the relationship between the amount of kelp classified and the tidal condition during each survey was plotted.

The imagery from five surveys between April 1st and May 31st were used in the analysis. Only lines from GW's farm were analyzed due to repeated defects in the generated orthomosaics along the HSU ProvidenSea farm lines. The best performing classifier was the binary threshold applied to the Red-Blue indexed orthomosaic (Table 1). The thresholds selected were unique to each survey's orthomosaic. The resulting kelp classifications from each survey are shown in Figure 2.

The area of classified kelp increased throughout time, however, on day 30 (May 1st) there is generally a peak in kelp (Figure 3). The tide during that survey is at the lowest amongst all the surveys, at 0.148 m. During the following survey (May 15th) the tide is the highest amongst all the surveys, at 1.266 m, and the area of classified kelp drops significantly for all the lines. On the final survey before the harvest, the tide is low again (0.179 m) but most lines still had less kelp than classified on May 1st. The greatest area of classified kelp is on line 2-1, with 23.6 m2 of kelp.

From repeated UAV surveys to monitor cultivated bull kelp, we found an effective method of analyzing kelp growth remotely, using UAV and a binary threshold classification method. This work, although successful in capturing growth also identified problematic factors in surveying lines on

Orthomosaic	Method	Accuracy in classfiying kelp		
		Producer	User	Kappa
Original RGB	Supervised	59%	91%	0.64
	Unsupervised	93%	85%	0.76
Red-Blue Index	Supervised	76%	76%	< 0.50
	Unsupervised	91%	91%	0.68
	Binary Threshold	88%	88%	0.76

Table 1: The results of the different classifications methods with the selected best performing one highlighted in yellow

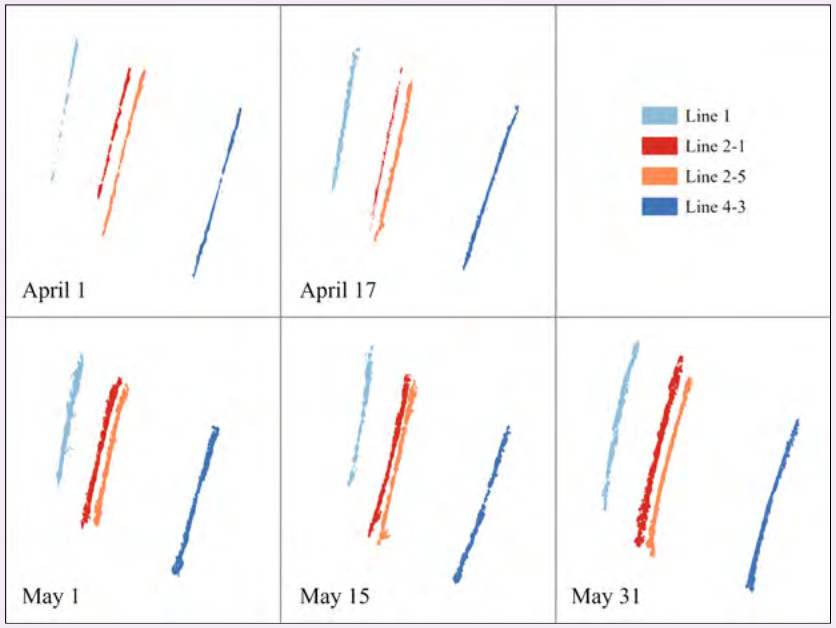

Figure 2: The classified kelp from the best performing classification method (binary threshold from the Red-Blue index) applied to each of the 5 surveys on the GW farm.

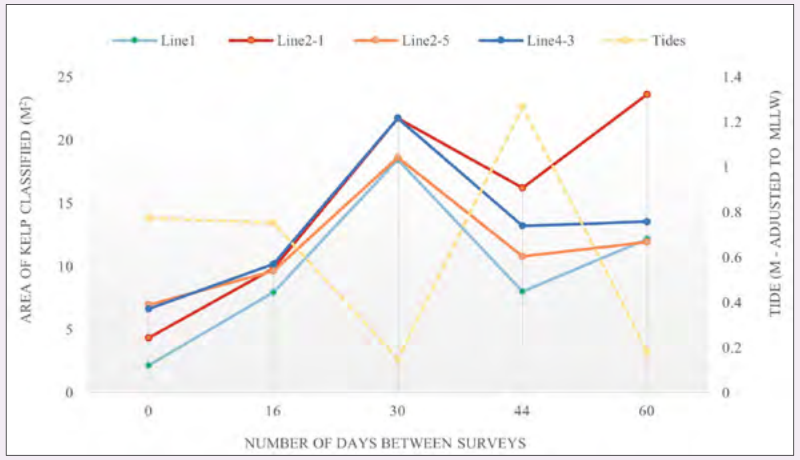

Figure 3: The area of classified kelp on each line throughout the 5 surveys, with the associated tide at the time of survey.

Click on either figure to enlarge.

continued on next page

a farm, namely the effect of tides on visible kelp. It was also discovered that creating the orthomosaic was only successful when there was enough kelp growth visible at the water's surface. A survey performed shortly after setting the seeded lines on the farms (March 11th, 2022) proved unsuccessful in the orthomosaic stage of processing and images capturing the HSU ProvidenSea lines, which were seeded later than GW lines, were also incapable of processing. The reduction in kelp area classified from the final survey (May 31st) may be a result of senescence of the kelp, observed during harvest.

In classifying, the supervised method was relatively unsuccessful on either the original RGB or the Red-Blue indexed orthomosaic, earning the lowest performance metrics. We had chosen to train a class based on obvious color differences in the buoys, however, based on the unsupervised classification results, the "shadow" adjacent to the floating kelp (likely from submerged kelp) was more spectrally significant. The unsupervised classification applied on both orthomosaics had a higher total producer and user accuracy, thus may have offered a better option for distinguishing kelp, but the lower kappa value indicates poor performance in distinguishing the other classes. Regardless, this method may be more suitable since accuracy in the other classes is less important in this work, and it took considerably less time. Adding more classes may improve the results.

ACKNOWLEDGEMENTS

Thank you to The Nature Conservancy for granting access to DroneDeploy Pro and for sharing information on best practices. We greatly appreciate the teams behind both kelp farms and the Humboldt Harbor District for making this work possible. We acknowledge the funding support of CSU Council on Ocean Affairs, Science & Technology and Cal Poly Humboldt in providing the UAV.

REFERENCES

Cavanaugh, Katherine C., Kyle C. Cavanaugh, Tom W. Bell, and Evan G. Hockridge. 2021. "An Automated Method for Mapping Giant Kelp Canopy Dynamics from UAV." *Frontiers in Environmental Science* 8 (February): 1–16. https://doi.org/10.3389/fenvs.2020.587354.

Choplin, Thierry, Charles Yarish, Robert Wilkes, Ellen Belyea, Shan Lu, and Arthur Mathieson. 1999. "Developing Porphyra/Salmon Integrated Aquaculture for Bioremediation and Diversification of the Aquaculture Industry." Journal of Applied Phycology 11. https://doi.org/10.1023/A:1008114112852.

Duarte, Carlos M. 2017. "Reviews and Syntheses: Hidden Forests, the Role of Vegetated Coastal Habitats in the Ocean Carbon Budget." *Biogeosciences* 14 (2): 301–10. https://doi.org/10.5194/bg-14-301-2017.

Gleason, Mary, Julie Zimmerman, James Ray, Rebecca Flores-, and Gina Contolini. 2021. "A Structured Approach for Kelp Restoration and Management Decisions in California." *The Nature Conservancy, Arlington, Virginia,* 54.

Graham, Michael H., Paul K. Dayton, and Jon M. Erlandson. 2003. "Ice Ages and Ecological Transitions on Temperate Coasts." *Trends in Ecology & Evolution* 18 (1): 33–40. https://doi.org/10.1016/S0169-5347(02)00006-X.

GreenWave. n.d. "GreenWave." Accessed June 4, 2022. https://www.greenwave.org/.

Huang, C., L. S. Davis, and J. R. G. Townshend. 2002. "An Assessment of Support Vector Machines for Land Cover Classification." *International Journal of Remote Sensing* 23 (4): 725–49. https://doi.org/10.1080/01431160110040323.

Jensen, John, John Estes, and Larry Tinney. 1980. "Remote Sensing Techniques for Kelp Surveys." *Photogrammetric Engineering and Remote Sensing 46* (6): 743–55. https://www.asprs.org/wp-content/uploads/pers/1980journal/jun/1980_jun_743-755.pdf.

Joyce, K. E., S. Duce, S. M. Leahy, J. Leon, and S. W. Maier. 2019. "Principles and Practice of Acquiring Drone-Based Image Data in Marine Environments." *Marine and Freshwater Research* 70 (7): 952. https://doi.org/10.1071/MF17380.

Kim, Jang K., Charles Yarish, Eun Kyoung Hwang, Miseon Park, and Youngdae Kim. 2017. "Seaweed Aquaculture: Cultivation Technologies, Challenges and Its Ecosystem Services." ALGAE 32 (1): 1–13. https://doi.org/10.4490/algae.2017.32.3.3.

McDowell-Group. 2017. "Economic Analysis to Inform a Comprehensive Plan Phase 2." https://afdf.org/research-library/ami-phase-2-economic-analysis-to-inform-a-comprehensive-plan.

Ray, J., T.A. McHugh, M. W. Esgro, K. Elsmore, and J. Freiwald. 2022. "Project 1-Bull Kelp Restoration in the Mendocino Region of Northern California. In Kelp Restoration Guidebook: Lessons Learned from Kelp Projects Around the World." Sacramento, CA. https://kelpforestalliance.com/TNC-KFA-Kelp-Guidebook-2022.pdf.

Rogers-Bennett, L., and C. A. Catton. 2019. "Marine Heat Wave and Multiple Stressors Tip Bull Kelp Forest to Sea Urchin Barrens." *Scientific Reports* 9 (1): 15050. https://doi.org/10.1038/s41598-019-51114-y.

Springer, Yuri P., Cynthia G. Hays, Mark H. Carr, and Megan R. Mackey. 2007. "Ecology and Management of the Bull Kelp, Nereocystis Luetkeana: A Synthesis with Recommendations for Future Research." https://www.lenfestocean.org/~/media/legacy/lenfest/pdfs/springer_underlying_report_0.pdf.

Stopha, Mark. 2020. "Alaska Kelp Farming: The Blue Revolution." Alaska Department of Fish and Game. 2020. https://www.adfg.alaska.gov/index.cfm?adfg=wildlifenews.view_article&articles_id=949#:~:text=Kelp farming is in its,stimulate interest in kelp farming.

Troell, M, P Rönnbäck, C Halling, N Kautsky, and A Buschmann. 1999. "Ecological Engineering in Aquaculture: Use of Seaweeds for Removing Nutrients from Intensive Mariculture." *Journal of Applied Phycology* 11: 89–97.

Turner, N. J. 2001. "Coastal Peoples and Marine Plants on the Northwest Coast." Edited by J. W. Markham and A. L. Duda. *26th Annual Conference of the International Association of Aquatic and Marine Science Libraries and Information Centers,* February, 67–76. https://darchive.mblwhoilibrary.org/handle/1912/2545.

Ward, M., T.A. McHugh, K. Elsmore, M. Esgro, J. Ray, M. Murphy-Cannella, I. Norton, and J. Freiwald. 2022. "Restoration of North Coast Bull Kelp Forests: A Partnership Based Approach." Marina Del Rey. https://www.opc.ca.gov/webmaster/ftp/pdf/agenda_items/20220614/Item5_Exhibit_A_Mendocino_County_Kelp_Forest_Restoration_Project_final_report.pdf.

AUTHORS:

Hannah Joss, MSc.
Student
Humboldt State University
Hannah.Joss@humboldt.edu

Dr. James Graham
Associate Professor of Geospatial Science
Humboldt State University
James.Graham@humboldt.edu

Dr. Rafael Cuevas Uribe
Associate Professor of Fisheries Biology
Humboldt State University
Rafael.CuevasUribe@humboldt.edu

Examining Spatial Accessibility to Primary Healthcare Facilities in Los Angeles County

Spatial accessibility has been defined as the relative ease by which the local residents at a given location can obtain a service that is provided at multiple facilities (Langford, Higgs, and Fry 2016). Spatial accessibility can quantify and highlight links, gaps, and inequalities between population centers (i.e., demand points) and urban facilities (i.e., supply locations), emphasizing the uneven spatial distribution of supply facilities' locations and population points. In light of this, measuring spatial accessibility to healthcare services has received growing attention from the public health and geospatial research communities.

Inadequate access to primary healthcare practitioners has been recognized as a key facilitator of overall population health, as poor access may result in avoidable health consequences (Bauer and Groneberg 2016). Within this context, it is essential for any healthcare program to guarantee an accessible network of primary healthcare practitioners. The effectiveness of such programs strongly relies on precise and reliable measures of spatial accessibility patterns so that the regions with poor access to primary healthcare providers may be identified. Measures of spatial accessibility can be used to direct federal and municipal resources and funds to the most underserved neighborhoods and serve as a benchmark for future service planning. (Langford, Higgs, and Fry 2016).

Various procedures and metrics have been proposed and developed to assess spatial access, with the Two-Step Floating Catchment Area (2SFCA) method being one of the most popular and gaining prominence in the geospatial sciences. Developed by Luo and Wang (2003), the 2SFCA methodology is a derivative of the gravity model. It tackles two key features of spatial accessibility: i) proximity to service provider facilities (e.g., healthcare facilities) and ii) availability and capacity of services over space. In essence, the 2SFCA technique computes a spatial accessibility metric that is a ratio of supply and demand in a given geography, computing where these two interact according to the distance decay concept (Wang 2018).

As suggested by the name of the technique, the 2SFCA is a two-step procedure. The first step concentrates on the service providers' facilities by defining a catchment area (with a predetermined distance/time) for service providers and calculating the total population within each catchment area. This step then calculates a ratio of provider-to-population for each facility location. The second step focuses on the population centers. Here the catchment areas are generated for each population center, and the sum of all provider-to-population ratios of the facilities that fall within the catchment area is calculated. The sum for each population center yields a metric that measures the relative spatial accessibility for each population (demand) location.

The generalized 2SFCA applies the distance decay function to both steps of the method, which has a well-established theoretical foundation in spatial gravity models. Accordingly, the generalized 2SFCA can be represented as follows:

$$\text{Step 1:} \quad R_j = \frac{S_j}{\sum_{k\in[d_{kj}\le d_0]} P_k . f(d_{kj})} \quad \text{for } j = 1,2,\dots,n \tag{1}$$

$$\text{Step 2:} \quad A_i = \sum_{j\in[d_{ij}\le d_0]} R_j . f(d_{ij}) \quad \text{for } i = 1,2,\dots,m \tag{2}$$

where A_i denotes the spatial accessibility index at the population location i (demand point i), where larger values of A_i indicate a higher (better) accessibility to provider locations and R_j is the provider-to-population ratio at each provider location j. n is the total number of provider/supply locations [e.g., primary care locations] where $j = 1,2,\dots,n$ and m represents the total number of population locations (demand points) where $i = 1,2,\dots,m$. S_j denotes the capacity of the supply at provider location j (e.g., number of primary healthcare physicians at location j). P_k represents the population at the location k that falls within the catchment (i.e., $d_{ki} \le d_0$). d_0 denotes user-defined travel time threshold (catchment size). And finally, $f(d_{ki})$ represents a distance decay function. In this research, we applied a Gaussian function that has been utilized widely in earlier studies (for example see: Tao, Cheng, and Liu 2020):

$$f_3(d_{ij}) = \begin{cases} \frac{e^{(-1/2)\times(d_{ij}/d_0)^2} - e^{(-1/2)}}{1-e^{(-1/2)}}, d_{ij} \le d_0 \\ 0, d_{ij} \ge d_0 \end{cases} \tag{3}$$

This research focuses on quantifying spatial accessibility to primary healthcare facilities for the general population in Los Angeles County, California. In this study, we compiled

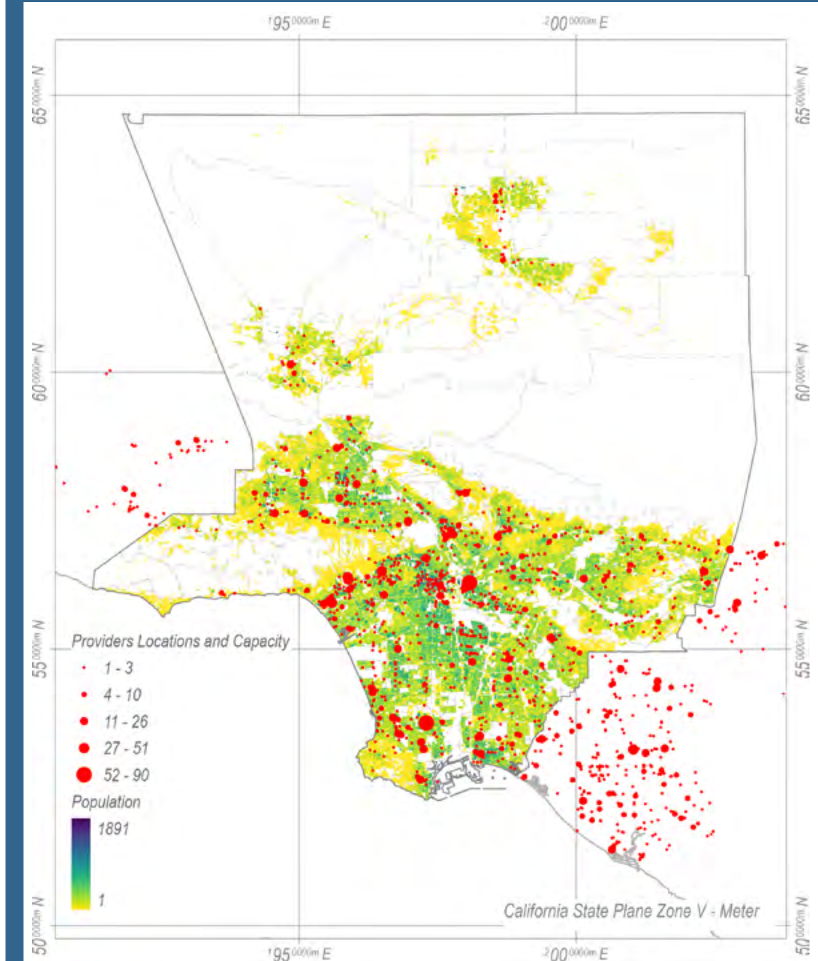

Figure 1: Spatial Distribution of Population and the Primary Healthcare Centers in Los Angeles County.

Click on image to enlarge.

continued on next page

TOC

and used three different datasets: i) primary healthcare physicians/facilities locations, ii) population locations, and iii) transportation network datasets. The list of primary healthcare providers and facilities representing the supply locations was obtained from the Center for Medicare and Medicaid Services portal ("Medicare Provider Utilization and Payment Data: Physician and Other Practitioners | CMS" n.d.). On the demand side, Census Block Groups weighted mean centers of the population have been used to represent the population centers within the county. Finally, the transportation network dataset was created using ESRI North American Road dataset in ArcGIS Pro Network Analyst Extension. Figure 1 shows the distribution of the population and the locations and capacity of primary healthcare services within Los Angeles county. We chose a 30-minute catchment area (d_0 in equations 1-3) for modeling the relationship between population and the primary physicians' locations which conforms with previous research in healthcare spatial accessibility (Hu et al. 2020; Lin et al. 2021).

Figure 2 shows the standardized variation of the spatial accessibility areas measures across the study area. The areas with higher accessibility scores (better or easier spatial access to primary care physicians) are concentrated in the core center of Los Angeles county, around the downtown area. This result reveals a higher accessibility measure around major arteries within the county. There are two visible higher accessibility along the North-South corridor of Interstate Highway 405 and Interstate Highway 110. Moreover, there are higher accessibility regions along the East-East corridor of Interstate Highway 10 and Ventura Freeway. In contrast, the lowest spatial accessibility scores are clustered primarily in periphery communities. These areas include the Canyon County and Humphreys neighborhoods of Santa Clarita, the Pearland neighborhood of Palmdale, and the Sunland-Tujunga neighborhood of Los Angeles.

The 2SFCA proved to be a technique easily implemented within GIS, requiring only a few datasets. The technique produced simple and easily interpretable indices of supply-to-demand ratios. This technique using the same datasets can be used and applied in other scenarios and locations, specifically in developing countries.

ACKNOWLEDGMENT

We would like to thank the College of Social and Behavioral Science at CSUN for funding this project.

REFERENCES

Bauer, Jan, and David A. Groneberg. 2016. "Measuring Spatial Accessibility of Health Care Providers – Introduction of a Variable Distance Decay Function within the Floating Catchment Area (FCA) Method." *PLOS ONE* 11 (7): e0159148. https://doi.org/10.1371/journal.pone.0159148.

Hu, Shuju, Wei Song, Chenggu Li, and Jia Lu. 2020. "A Multi-Mode Gaussian-Based Two-Step Floating Catchment Area Method for Measuring Accessibility of Urban Parks." *Cities* 105: 102815.

Langford, Mitchel, Gary Higgs, and Richard Fry. 2016. "Multi-Modal Two-Step Floating Catchment Area Analysis of Primary Health Care Accessibility." *Health & Place* 38: 70–81.

Lin, Yan, Christopher Lippitt, Daniel Beene, and Joseph Hoover. 2021. "Impact of Travel Time Uncertainties on Modeling of Spatial Accessibility: A Comparison of Street Data Sources." *Cartography and Geographic Information Science* 48 (6): 471–90.

"Medicare Provider Utilization and Payment Data: Physician and Other Practitioners | CMS." n.d. Accessed July 6, 2022. https://www.cms.gov/Research-Statistics-Data-and-Systems/Statistics-Trends-and-Reports/Medicare-Provider-Charge-Data/Physician-and-Other-Supplier.

Tao, Zhuolin, Yang Cheng, and Jixiang Liu. 2020. "Hierarchical Two-Step Floating Catchment Area (2SFCA) Method: Measuring the Spatial Accessibility to Hierarchical Healthcare Facilities in Shenzhen, China." *International Journal for Equity in Health* 19 (1): 1–16.

Wang, Fahui. 2018. "Inverted Two-Step Floating Catchment Area Method for Measuring Facility Crowdedness." *The Professional Geographer* 70 (2): 251–60.

AUTHOR

Soheil Boroushaki
Associate Professor, Department of Geography
California State University, Northridge
soheil.boroushaki@csun.edu

Negin Rezaei
Graduate Student, Department of Geography
California State University, Northridge
negin.rezaei.977@my.csun.edu

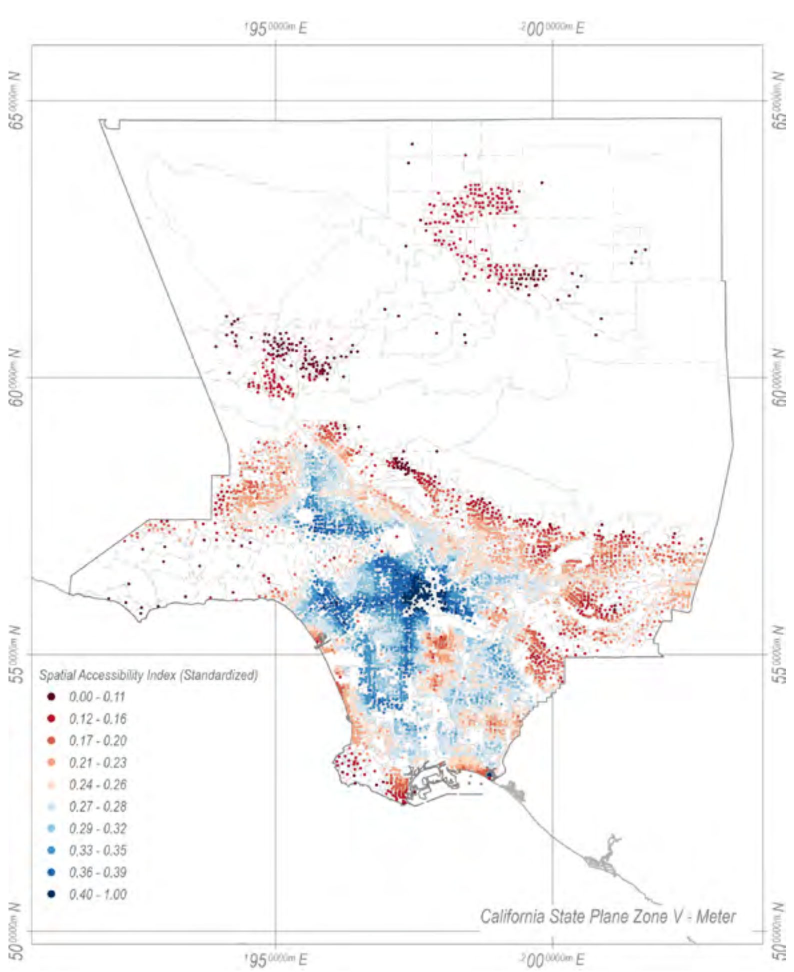

Figure 2: Spatial Accessibility to Primary Healthcare Facilities for Census Block Groups in Los Angeles County.

Click on image to enlarge.

csugis.sfsu.edu

TOC

Ecological Assessment of Restored Wetlands in California Central Valley Integrating UAS and Survey Data

California's Central Valley has lost over 95% of all depressional wetlands and 98% of all riparian habitats, resulting in reduced water availability and quality (Garone 2011). Drained wetland areas, which have been predominantly replaced by agricultural croplands, cover roughly 3 million ha, over half of the Central Valley (CV). Decades of flood control measures, including the construction of countless reservoirs and water delivery canals has resulted in a heavily altered landscape experiencing skyrocketing water demands, usually to the detriment of natural water bodies including the state's critically sensitive wetlands and streams. Every acre-foot of water is accounted for, and most remaining wetlands are managed under strict hydrological regimes (Central Valley Joint Venture 2006). Water flowing through the dense network of channels crisscrossing the CV is used and re-used for irrigation purposes, accumulating ever increasing concentrations of agrochemicals that diminish water quality further downstream. Many wetland habitats are recharged with this degraded water, which has had seri-ous negative impacts on wetland dependent wildlife (Rennie, 1996). This study sought to examine the relationship between restored wetland quality and adjacent land use by applying spatial analysis techniques to quantify the number and density of drainage channel nodes to fertilized cropland.

Over-fertilization, soil erosion and grazing, and agricultural runoff are major contributors to surface and groundwater contamination, posing serious threats to human and ecosystem health. To mitigate the effects of agriculture on surface water, the U.S. Department of Agriculture-Natural Resource Conservation Service (USDA-NRCS) encourages landowners to create, restore or enhance wetlands to provide ecosystem services such as water filtration, soil amendment, carbon sequestration, groundwater replenishment, and wildlife habitat (NRCS 2019). Few studies have examined water quality impacts on surface water from a spatial perspective. A team of scientists from Cal Poly Humboldt, led by Dr. Sharon Kahara, a wetlands and wildlife biologist investigated links between land use, water quality and wetland dependent wildlife including waterfowl and amphibians. The purpose of their research was to characterize and model restored wetland ecological functions building upon 15 years of data collected in the CV. Using the dynamic process modeling tool STELLA ® (Systems Thinking and Experimental Learning Laboratory with Animation), Dr. Kahara and her team simulated restored wetland hydrology and nutrient dynamics as a function of vegetation coverage and growth. At the model's core is a simple mass balance of daily hydrological inputs and outputs that include surface flows, precipitation and evapotranspiration (Fig. 1). The model in its present form does not account for groundwater exchange as there is little evidence of this exhibiting within the study area, but may become more apparent along the margins of the CV.

The model assumes that water, the primary medium in which nutrient transformations take place, flows evenly across the restored wetland with no preferential flow or channeling patterns. All vegetation is assumed to be rooted and in contact with water resources, however growth is restricted only to times when water is present. The hydrology sub-models calculate the water level in each wetland (as the volume of water per square-meter of surface area) based on surface inflows, outflows, precipitation, and evaporation. Modeled water depths aligned well with empirical data collected at over 12 wetland sites between 2016-2020 (Fig. 2). Modeled hydrology emphasized the strong influence of artificial hydrology in restored wetlands of the CV as water depths could not be explained by natural precipitation, evaporation or overland flows alone. Such over-reliance on human intervention to maintain hydrology is a major shortcoming of restored wetland hydrology and reiterates previous findings that indicate a strong influence of California's water regulators on wetland ecosystem services (Kahara et al., 2022).

Unmanned aerial system (UAS) imagery was also monitored at eight privately managed restored wetlands in three regions of the Central Valley (Sacramento, Delta, and San Joaquin), once in the summer and fall, from 2020 to 2022 using a DJI Phantom 4 PRO (SZ DJI Technology Co., Ltd., Nanshan, China) flying at an average height of 120 m above ground height (AGH) with side and front overlaps of at least 80%. Ground Sample Distance (GSD) was 4 cm/px. Autonomous flight path plans for the aerial image collections were designed using the DroneLink application. A light drone (DJI Mavic Mini was flown at lower elevation (around 10 m AGH) for reconnaissance and assisted in vegetation species identification (view video compilation here). The product UAS image collection was processed to create orthomosaic images using the ortho mapping workspace within the ArcGIS Pro software (Esri, Redlands. California, USA). During this processing and prior to any orthomosaic creation and subsequent analysis, the adjustment tool was run to “stitch” the images to ensure accurate geometric transformation models (UCANR-IGIS, 2020).

Interannual phenological changes in wetland vegetation were calculated for 3-band (RGB data) UAS imagery collected, applying the Visible Atmospherically Resistant Index (VARI) as follows:

$$VARI = (Green - Red) / (Green + Red - Blue)$$

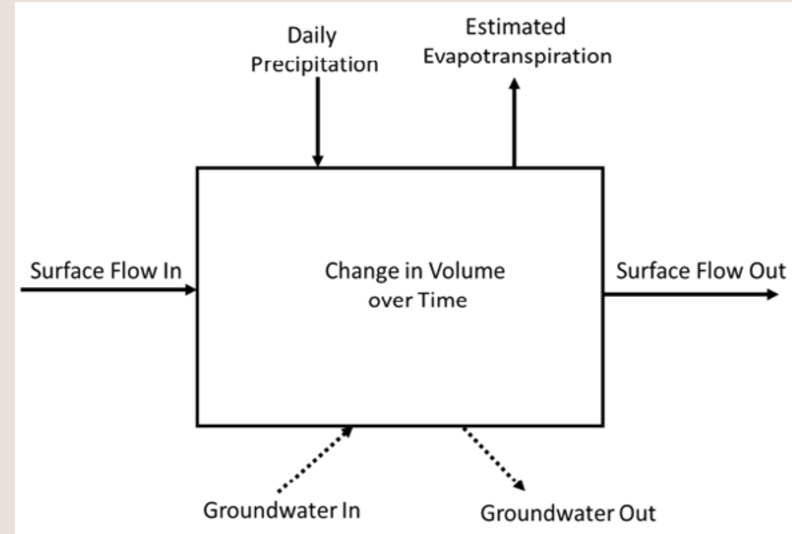

Figure 1: Wetland budget indicating typical inputs and outputs of a restored wetland in California's Central Valley.

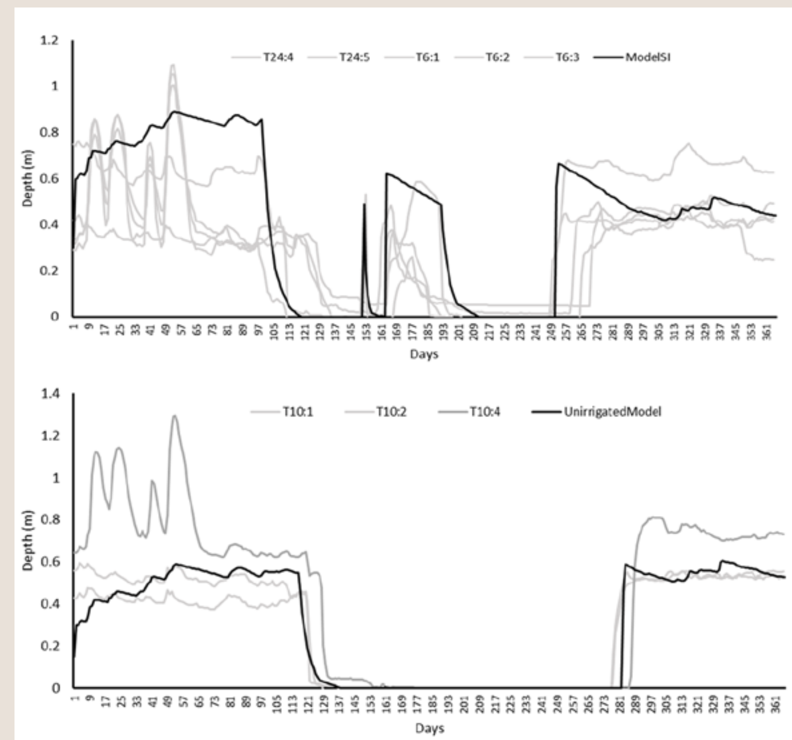

Figure 2: Modeled and empirical irrigated (A) and unirrigated (B) wetland water depths (black line) in Colusa, California from January 1, 2017 to December 31, 2017. Peak flows observed in measured water depths are likely the result of overland flows from the Colusa Weir due to above average precipitation in the early part of the year.

Click on image above to enlarge

continued on next page

TOC

The VARI estimates the fraction of vegetation in a scene with low sensitivity to atmospheric effects (Eng et al., 2019). This vegetation index formula was chosen for its ability to detect changes due to biomass accumulation and sensitivity to the amount of chlorophyll in leaves, while remaining accessible as images derived from a consumer grade RGB drone camera meets the requirements for VARI utilization (Eng et al., 2019).

The objective of this study was to characterize and quantify seasonal differences in vegetation coverage at the Sugiyama wetland easement in San Joaquin using a simple vegetation index that derived from the UAS imagery. Results of the VARI assessment at the Sugiyama wetland easement in San Joaquin are shown in Fig. 3. The vegetative cover at the Sugiyama wetland easement is about 8.82% (3.47 ha) and 1.07% (0.42 ha) during summer and fall 2021 respectively. Less vegetation in the fall compared to the summer is likely the result of vegetation removal efforts (mowing) conducted by the landowners. Vegetation removal prior to fall flooding, referred to as moist soil management, is a recommended pre-flooding treatment in easements managed for wintering waterfowl (Hagy and Kaminski, 2012).

This project also supported undergraduate and graduate students in acquiring field data collection and provided preliminary remote sensing experience. Dr. Madurapperuma's intermediate remote sensing class (GSP 326) at California Polytechnic State University-Humboldt used a semi-automated workflow (i.e. Object-Based Image Analysis) to produce an autonomous count of waterfowl while distinguishing three separate bird species in Colusa County, California using UAS imagery. The student's project findings were showcased at the American Association of Geographers (AAG) Annual Meeting in 2021 (Hernandez et al., 2021), and the Annual Science Research Sessions at the South-Eastern University of Sri Lanka (Fisher et al., 2022). Flourishing waterfowl populations, particularly in late fall and early winter months, on restored wetlands have been linked to increased nutrient inputs (Kim et al., 2020), thus warranting this use of UAS for bird surveying.

Ongoing analysis focuses on the role of ecological factors at multiple spatial scales on native and invasive amphibian occupancy. The project is a graduate research thesis that employed landscape ecology and environmental DNA techniques to clarify the roles adjacent land use and site-specific habitat characteristics affect occupancy dynamics of native species.

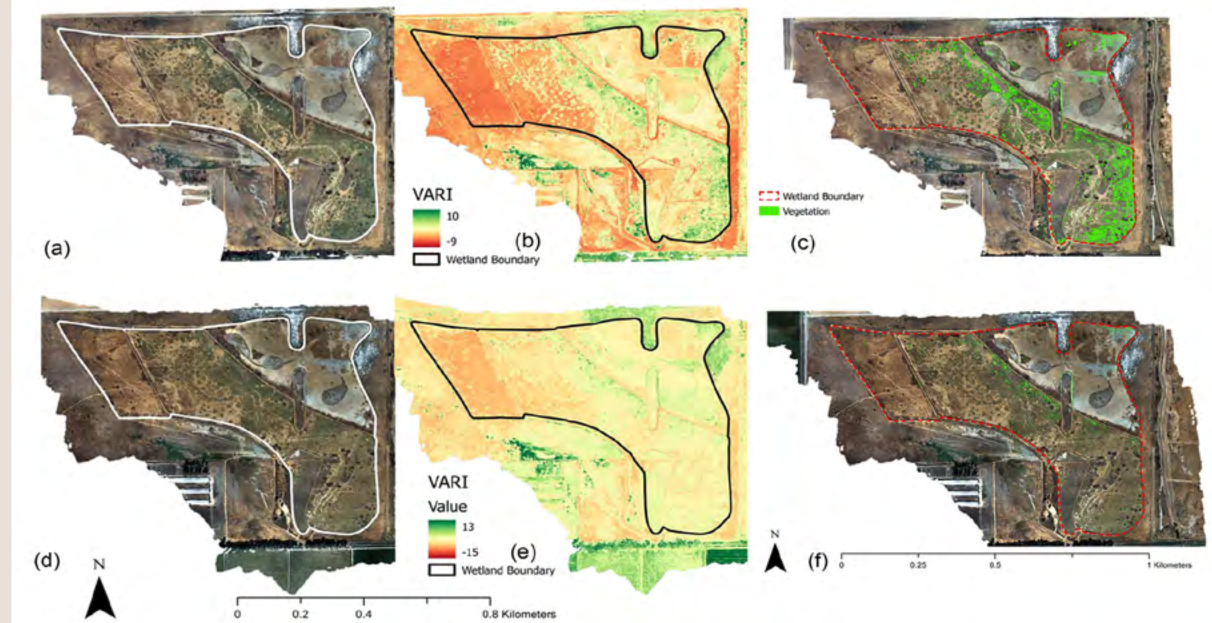

Figure 3: UAS images at the Sugiyama wetland easement in San Joaquin during summer and Fall 2021: summer orthomosaic, VARI, and % vegetation cover (a, b & c), fall orthomosaic, VARI, and % vegetation cover (d, e & f) Higher values (green) indicate healthy vegetation while low values (red) indicate bare soil, road or dead vegetation.

Click on image to enlarge

REFERENCES

Central Valley Joint Venture [CVJV]. (2006). Central Valley Joint Venture implementation plan-conserving bird habitat. U.S. Fish and Wildlife Service, Sacramento, California, USA.

Eng, L.S., Ismail, R., Hashim, W., Baharum, A. (2019). The use of VARI, GLI, and VIGREEN formulas in detection vegetation in aerial images. International Journal of Technology 10(7): 1385-1394.

Fisher, J., Marlin, K., Pickering, A., Scaroni, L., Weisgrau, A.S., Kahara, S.N., Hernandez, K.B., Paredes, E.J., Lamping, J.E., Nijamir, K., Manamperi, J.P.J., Kuruppuarachchi, K.A.J.M. & Madurapperuma B.D. (2022). Bird counts in California's Central Valley wetlands using object based image analysis. *Proceedings of the 11th Annual Science Research Sessions,* FAS, SEUSL, Sri Lanka, 15th November 2022, p.34. https://www.seu.ac.lk/asrs2022

Garone, P. (2011). The fall and rise of wetlands of California's Great Central Valley. University of California Press, Berkeley, California, USA.

Hagy H.M., & Kaminski, R.M. (2012).Winter food and waterfowl dynamics in managed moist-soil wetlands of the Mississippi Alluvial Valley. *The Wildlife Society Bulletin* 36: 512–523. https://wildlife.onlinelibrary.wiley.com/doi/10.1002/wsb.165

Hernandez, K., Fisher, J., Marlin, K., Pickering, A., Scaroni, L., W eisgrau, A., Madurapperuma, B., Kahara, S. & Lamping, J. (2021). Use of sUAS imagery for surveying waterfowls in a managed wetland in Colusa County. *Annual Meeting American Association of Geographers,* 10th April 2021.

Kahara, S. N., Madurapperuma, B. D., Hernandez, B. K., Scaroni, L., & Hopson, E. (2022). Hydrology and Nutrient Dynamics in Managed Restored Wetlands of California's Central Valley, USA. Water, 14(21), 3574.

Kim, S., Jeong, J., Kahara, S. N., & Kiniry, J. R. (2020). APEX simulation: Water quality of Sacramento Valley wetlands impacted by waterfowl droppings. *Journal of Soil and Water Conservation,* 75(6), 713-726.

Natural Resource Conservation Service [NRCSb]. (2019). Conservation Practices. https://www.nrcs.usda.gov/wps/portal/nrcs/detailfull/national/technical/cp/ncps/?cid=nrcs143_026849#U. Accessed June 2019.

Rennie, S.M. 1996. Selenium in San Joaquin Valley Agricultural Drainage: A Major Toxic Threat to Fish and Wildlife Inadequately Addressed by the Central Valley Project Improvement Act, 27 Pac. L. J. 303 Available at: https://scholarlycommons.pacific.edu/mlr/vol27/iss2/6

University of California Division of Agriculture and Natural Resources Informatics and GIS [UCANR-IGIS]. (2020). Processing UAV Images with ArcGIS Pro. https://docs.google.com/document/d/1m5DLIWly-eptquSmN7hGZcou6vtQ0pBkiMOqrplyrios/edit. Accessed October 2022.

AUTHORS

Buddhika Madurapperuma, Ph.D.
Research Associate, Department of Forestry, Fire, and Rangeland Management
Cal Poly Humboldt University
bdm280@humboldt.edu

Sharon Kahara, Ph.D
Assistant Professor, Department of Biology and Environmental Science
University of New Haven
300 Boston Post Road,
West Haven, 06516, CT, USA

Luke Scaroni, B.A.
Graduate Student, Department of Geography, Environment, & Spatial Analysis
Cal Poly Humboldt University
ls291@humboldt.edu

Breana Hernandez, B.S.
Graduate Student, Department of Wildlife,
Cal Poly Humboldt University
kbh26@humboldt.edu

Elmer Paredes, B.S.
Graduated, Department of Forestry, Fire, and Rangeland Management
Cal Poly Humboldt University
ejp9@humboldt.edu

A Web-Based Multicriteria Spatial Decision Support System (SDSS) for Water Division Strategies

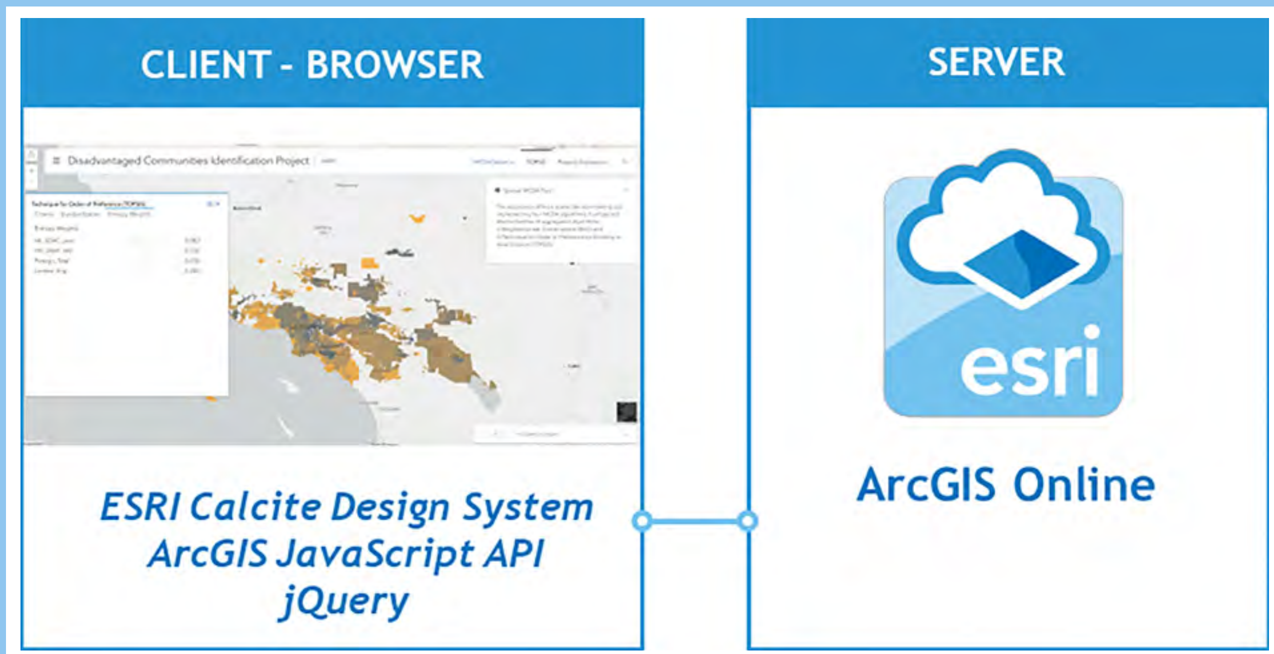

Figure 1: WebGIS-MCDA Application System Architecture.

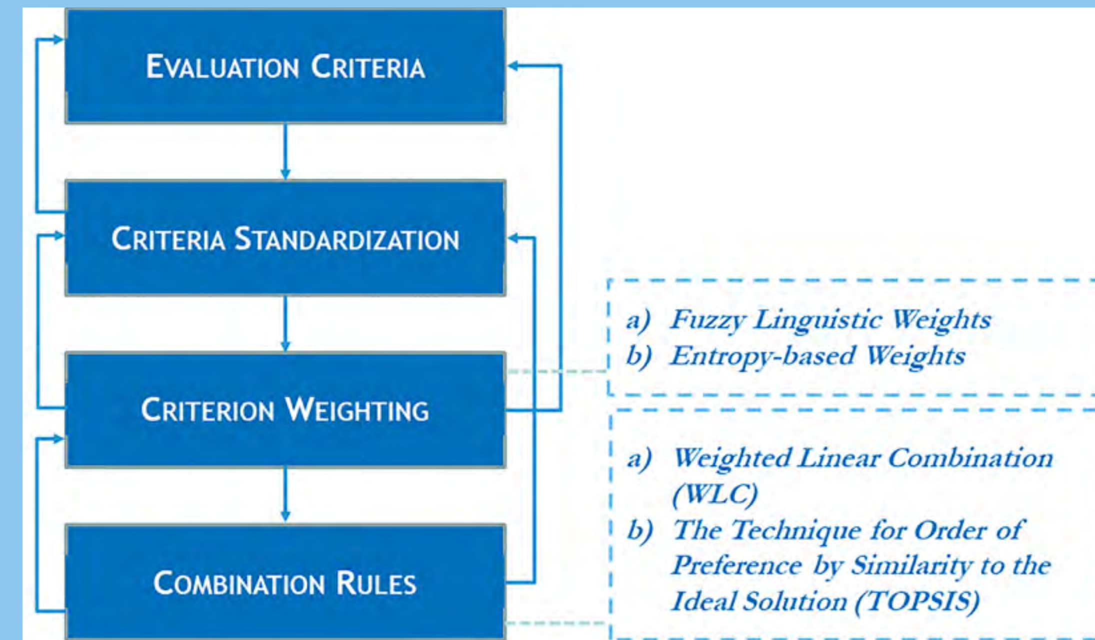

Figure 2: WebGIS-MCDA Application Process Flow.

Disadvantaged communities refer to those geographical areas that are heavily burdened by and suffer disproportionately from a combination of socio-economical, health, and environmental factors. Identifying disadvantaged communities remains the main objective of most urban and regional development planning efforts and policy-making to allocate and direct state and local governments' resources, funds, and subsidies. Within this context, the main objective of these types of spatial decision-making problems would be revitalizing disadvantaged communities by allocating resources to ensure sustainable development and environmental justice (California Office of Environmental Health Hazard Assessment 2017).

Within this context, Water Service Providers (WSPs) areas can sometimes be considered at a disadvantage in communities that lack access to adequate water resources and infrastructure. This can be particularly true in low-income or marginalized regions where water supply and treatment systems may be outdated or poorly maintained. Water Service Providers in disadvantaged communities face significant challenges in ensuring access to safe and reliable water supplies. Addressing these challenges will require a collaborative effort among stakeholders, including water providers, government agencies, and community members. Identifying, prioritizing, and ranking disadvantaged WSPs is paramount to facilitate their development better to serve their community with safe and reliable water.

Designating and identifying disadvantaged communities by nature is, in fact, a geospatial decision problem involving a broad set of evaluation criteria. Spatial decision problems, most often, involve a set of multiple, conflicting, and incommensurate evaluation criteria. The set of criteria in these problems is involved in the process of evaluation, ranking, and selection of the location alternative(s) that best serve the decision-making objectives. Within this context, spatial decision analysis or a GIS-based multicriteria decision analysis (MCDA) can be defined as a procedure to aggregate geospatial evaluation criteria and their relative importances into a final solution map. The solution map, in turn, can offer appropriate and valuable information and give insight into the decision-making problem. The integration of GIS and MCDA facilitates the decision-making process by allowing the participants (planners, administrators, or local citizens) to explore different aspects of the decision problem and articulate their preferences and judgments. In this setting, MCDA provides a mechanism for expressing decision-makers' knowledge and priorities over the spatial problem for generating a rank order of alternatives in such a way that a compromise solution is identified. Implementing a web-based GIS and aggregating MCDA techniques can create a distributed and possibly collaborative environment. WebGIS-MCDA can provide an interactive tool for users to explore maps and spatial alternatives and their attributes and easily express their opinions about the spatial decision problem. Such environments enable decision-makers (experts or the general public) to input their preferences regarding the spatial problem based on different times – different locations of the spatial-temporal dimensionality of spatial decision-making (Boroushaki and Malczewski 2010).

This project focuses on the implementation of a web-based multicriteria spatial decision support system (WebGIS-MCDA) for evaluating, prioritizing, and ranking a number of Water Service Providers within southern California in such a way that disadvantaged regions could be identified. The web-based decision tool has been designed and developed as a proof of concept on how MCDA techniques can be utilized for these types of spatial decision-making where the spatial units represent Water Service Providers (WSPs), as this project was contracted and supported by the CSU's Water Resource and Policy Initiatives (WRPI). The WebGIS-MCDA application uses a client-server architecture approach to web-based GIS. It employs the ESRI Calcite Design System and ArcGIS JavaScript API on the client side and utilizes ArcGIS Online and its capabilities on the server side. The additional functionalities of MCDA techniques have been developed using a combination of JavaScript and jQuery (Figure 1).

continued on next page

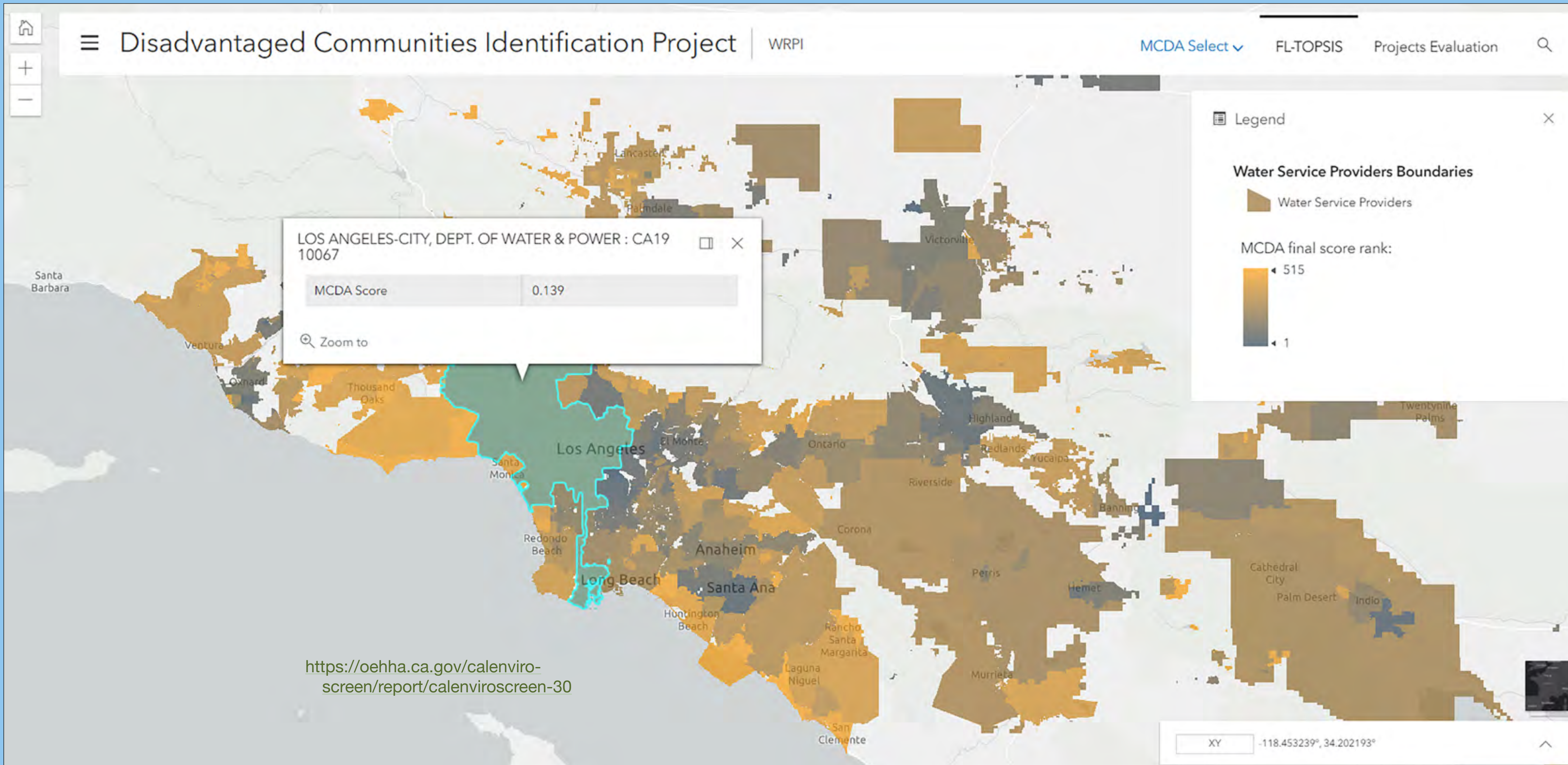

Figure 3: WebGIS-MCDA Application User Interface.

All the geographic data (WSP boundaries and attributes) is stored on ArcGIS Online as a feature layer. There are 515 WSPs considered in this project, with a set of 44 evaluation criteria that can be used in the decision-making process. The evaluation criteria cover a range of demographic and socio-economical attributes. The WSPs' boundaries and their attribution have been created, compiled, and maintained by the Center for Geospatial Science and Technology at the California State University, Northridge.

The WebGIS-MCDA application facilitates the following major steps of spatial decision-making: i) selection of the evaluation criteria; ii) standardization of the criteria; iii) assigning criteria weights; and finally, iv) aggregating the evaluation criteria based on their relative weights using a decision rule or multicriteria decision algorithm (Figure 2). In this framework, two major techniques for assigning criteria weights have been implemented, a fuzzy linguistic weighting scheme and a data-driven entropy-based weights calculation. Moreover, two MCDA aggregation algorithms have been developed and implemented for data aggregation: i) Weighted Linear Combination (WLC) and ii) the Technique for Order of Preference by Similarity to the Ideal Solution (TOPSIS) (see Boroushaki 2017). Figure 3 shows the output ranking of the WSPs based on the selections and preferences of a hypothetical decision-maker. In this case, the lower the ranking, depicts the disadvantaged communities (water service provider regions). The preliminary testing and calibration of the implemented application are now complete, and the WebGIS-MCDA application will be developed into a more comprehensive decision-making tool in the next phase. The WebGIS-MCDA application can be accessed at https://www.csun.edu/~sboroushaki/WRPI/.

ACKNOWLEDGMENT

This material is based upon work supported by the CSU's Water Resource and Policy Initiatives (WRPI).

REFERENCES

Boroushaki, S. 2017. Entropy-based weights for multicriteria spatial decision-making. Yearbook of the Association of Pacific Coast Geographers, 79: 168-187.

Boroushaki, S., and J. Malczewski, 2010. Measuring consensus for collaborative decision-making: A gis-based approach. *Computers, Environment and Urban Systems*, 34(4), 322-332.

California Office of Environmental Health Hazzard Assessment. 2017. CalEnviroScreen 3.0. Retrieved May 15, 2021, from https://oehha.ca.gov/calenviroscreen/report/calenviroscreen-30

AUTHOR

Soheil Boroushaki
Associate Professor, Department of Geography
California State University, Northridge
soheil.boroushaki@csun.edu